INFLUENCE OF DIFFERENT PUMPING AND RECHARGING SCHEMES ON REGIONAL GROUNDWATER DRAWDOWN IN GROUNDWATER HEAT PUMP PROJECT
A Case on Anhui Fuyang People's Hospital

by

Jie YANG [a,b]***, Wei WANG*** [a]***, Lin HU*** [a]***, Yulan GAO*** [b]***, and Yuezan TAO*** [a*]

[a] School of Civil Engineering, Hefei University of Technology, Hefei, China
[b] Department of Architecture and Civil Engineering, West Anhui University, Lu'an, China

Original scientific paper
https://doi.org/10.2298/TSCI200614316Y

In the process of exploiting geothermal energy by groundwater heat pump, the dynamic equilibrium of regional groundwater drawdown is the basis for sustained operation of groundwater heat pump. In this paper, taking the groundwater heat pump project of Fuyang People's Hospital in Anhui, China as an example, a mathematical model is established and numerical simulation is carried out based on the hydrogeological conceptual model by using MODFLOW software. In addition, considering the pattern of same direction recharge, the intersect recharge, and the ratio of 90% and 100% reinjection, respectively, the area change of the drawdown funnel caused by the groundwater heat pump project and the recovery of the water level after the system stopped operation are analyzed. The results show that the funnel area of the pumping well under the 90% recharge ratio is greater than that of the 100% recharge, while the operation result of recharge well is opposite in the most adverse situation of the system with a production volume of 1440 m^3 *per day and continuous operation for 4 months. Furthermore, with the same reinjection ratio, the funnel area of the same direction recharge mode is larger than that of the intersect recharge mode in both pumping wells and recharge wells, and increases with the decrease of drawdown. Moreover, with the increase of recharge amount, while the water level of recharge well rises, there is a certain supplement and balance to the water quantity of the pumping well.*

Key words: groundwater heat pump, drawdown, numerical simulation, recharge ratios, funnel area

Introduction

Currently, due to the large amount of CO_2 and other GHG in the use of non-renewable energy such as coal, oil and natural gas, the global climate warming and the worsening of ecological environment have been widespread concerns in the world for energy conservation, environmental protection and sustainable use of energy [1, 2]. Geothermal is a new, renewable, clean and pollution-free energy which has attracted increasing attention by people [3-5]. As an important geothermal energy extraction and utilization technology, groundwater heat pump (GWHP) is developing rapidly in China and other parts of the world due to its advantages of resource saving, low carbon emission, environmental friendliness, and economic efficiency [6-8].

[*] Corresponding author, e-mail: 2019030008@mail.hfut.edu.cn

The GWHP is a central heating and cooling system that absorbs solar energy and geothermal energy from shallow groundwater [9, 10]. In winter, the formation can provide higher temperature, and the groundwater is pumped to the surface to heat the building space, while the cold water is pumped back to the aquifer after heat transfer. In summer, relatively low temperature shallow groundwater is pumped to the surface for heat exchange and cooling, and hot water is poured back to the ground [11-13]. In theory, the underground energy of the region can be kept roughly in balance during the whole operation cycle [14].

However, in the process of pumping and recharging, with the rise and fall of temperature and the transfer and exchange of energy, the work of the heat pump system can be regarded as the hydrothermal coupling between the groundwater seepage field and the temperature field. Many scholars have done a lot of research on heat transfer characteristics and performance parameters of GWHP. Huchtemann and Muller [15] investigated the heat transfer characteristics of building heating in a water source heat pump project of an office building, the results showed that the flow in the pumping well and the diameter of the well pipe had significant effects on the outlet temperature of the system. Noorollahi *et al.* [16] analyzed the main factors affecting the heat conduction, such as flow rate, geothermal gradient and particle structure. As a hot topic, some numerical models and heat transfer models have been applied to various engineering practices [17, 18]. Bidarmaghz *et al.* [19] developed a 3-D numerical model to study the influence of surface air temperature change on borehole heat exchanger (BHE), and analyzed the possible errors caused by surface air temperature fluctuation and other factors on the design of BHE.

Most previous studies focused on the temperature field, heat conduction and coupling model of GWHP [20, 21], but there are few researches on the influence of well pumping and recharge on regional groundwater drawdown in groundwater seepage field. However, the timely recovery and dynamic balance of groundwater level are the basis for the continuous operation of GWHP. Based on the aforementioned issues, the objective of this paper was to study the influence of different pumping and recharge schemes on the regional groundwater level and drawdown funnel area. Taking the GWHP project of Anhui Fuyang People's Hospital as an example, established a mathematical model according to the hydrogeological characteristics, then the visal MODFLOW software was used for numerical simulation. What's more, the area of the water level descending funnel or the reverse ascending funnel in the GWHP project under the various working conditions and the water level recovery after the system stops operation were analyzed by taking into account the same direction recharge mode, intersect recharge mode and the proportion of 90-100% recharge, respectively. Therefore, it is of practical significance to study different pumping and recharging schemes of GWHP for perfecting groundwater recharge technology and preventing land subsidence.

Materials and methods

Overview of the study area

Fuyang city in Anhui province, the southern part of the North China Plain and the western part of the Huaibei Plain, is located in the middle latitude of East China. Fuyang People's Hospital is a comprehensive top three hospitals, located in the northern part of the city, close to the Spring River urban landscape, covers an area of 125 acres, which including infectious building, logistics building, ward building, rehabilitation building, a total area of 135000 m^2 and investment of 51.2 million dollars. According to the climate characteristics and building energy-saving conditions, the project adopts GWHP in the air conditioning system design, in which the winter heating is all extracted from the geothermal water, the total heating load of the system is 6440 kW.

Hydrogeological characteristics

The study area is covered by 800-1500 m thick Neozoic loose strata and lies beneath the north China Huai River stratigraphic division. The regional stratigraphic distribution is shown in tab. 1.

Table 1. Summary of strata in the study area

Erathem	System	Thickness [m]	Main lithologic
Cenozoic erathem	Quaternary	>130	Interbed of silty fine sand, sub-sandy soil and sub-clay.
	Neozoic	550±	Semi-consolidated clay, clay, silty fine sand
		240±	Semi-consolidated silt, fine sand, gravel coarse sand and clay, sub-clay
	Palaeogene	>400	Siltstone, fine sandstone, mudstone
Mesozoic group	Cretaceous system	>200	Siltstone, mudstone, glutenite
Lower palaeozoic	Ordovician	150±	Dolomite, limestone
Lower Proterozoic		>300	Gneiss, granitic gneiss, amphibolic Amphibolic schist
		>1000	

From top to bottom, the Neozoic strata and their hydrogeological characteristics are the first layer which develop with phreatic aquifer, confined aquifer and clay layer is Quaternary, the buried depth of the bottom boundary of this formation is 180 m. The second layer is the upper Tertiary with low degree of consolidation in lithology, which belongs to loose rock in general. It can be divided into Guantao formation of Miocene series and Minghuazhen formation of Pliocene series, the thickness of which are 610 m and 606.7 m, respectively. The third layer is the Jieshou formation of the Paleogene system. The lithology of this formation is silty mudstone and fine sandstone, the unexposed thickness revealed by this drilling is 309.3 m and the drilling depth is 1526 m.

Geothermal water and mining design

The geothermal water demand of the project is determined by the total heating load. According to the pumping test data of the built geothermal wells in the area, the amount of thermal water required for design can be calculated:

$$Q_d = \frac{3600 P t_\mathrm{h}}{C\rho(T_r - T_0)} \tag{1}$$

where Q_d is the water intake flow of hot well, P – the total heating load, 6440 kW, C – the average heat capacity of hot water, 4.2 kJ/m^3°C, T_r – the pumping temperature, 50 °C, T_0 – recharge water temperature, 4 °C, t_h – the time in hours, 12 h, so the results show that Q_d is 1440 m^3 per day. In addition, the annual heating period of the project is four months from November to February of the following year.

Considering the hydrogeological conditions of the local section and the related exploration achievements of the project, the deep geothermal water of the Neogene Guantao formation and the Jieshou formation of the Paleogene were taken as the mining target, where the designed well depth was 1500 m. Besides, according to the pumping test of exploration wells, the water output capacity of a single well is 80 m^3 per hour, while the maximum water demand of the project is 120 m^3 per hour, so the geothermal mining design is two pumping wells and two recharge wells on the basis of the single well production capacity and total water requirement.

Model generalization and numerical simulation

Hydrogeological generalization

In view of the hydrogeological conditions of the region, the groundwater within the same parameter partition can be regarded as homogeneous, and the water flow conforms to Darcy's law. The simulated region is generalized into heterogeneous isotropy, and the groundwater flow state is 2-D unsteady flow, which is generalized into the known head boundary. Based on the analysis of the characteristics of strata, runoff and recharge, the regional geothermal water is mainly supplied laterally in the far distance in the natural state, but it can be supplied from outside the area through the infinite boundary in the mining state, the hydrogeological environment is relatively closed. Therefore, the target stratum is generalized as one layer: fine sandstone, fine medium sandstone with siltstone thin layer, the depth of distribution is about 890-1500 m.

Groundwater numerical model

Visual MODFLOW is a standard visual professional software system widely used in the world to simulate 3-D underground-water flow and solute transport, by solving finite difference equations, the value of grid points in each period can be obtained. In this study, according to the generalized hydrogeological conceptual model, the corresponding mathematical model was established as eqs. (2)-(4), and the process of pumping and recharge was simulated by visual MODFLOW to analyze its influence on the regional groundwater level:

$$\frac{\partial}{\partial x}\left(KM\frac{\partial H}{\partial x}\right)+\frac{\partial}{\partial y}\left(KM\frac{\partial H}{\partial y}\right)+W=\mu^{*}\frac{\partial H}{\partial t} \tag{2}$$

$$H\left(x,y,t\right)\Big|_{t=0}=H_{0}\left(x,y\right),\quad \left(x,y\right)\in D \tag{3}$$

$$H\left(x,y,t\right)\Big|_{\Gamma_1}=H_{1}\left(x,y,t\right),\quad \left(x,y\right)\in \Gamma_{1} \tag{4}$$

Boundary conditions and parameter assignment

Using the established numerical model, the time-space discretization is carried out, and the average water level of each point is calculated month by month. The study area is divided into about 2000 cells (twice locally encrypted) with an area of 2500 m^2. Besides, according to the hydrogeological conceptual model, it is simplified to one layer vertically.

The setting of boundary conditions refers to the heating projects around which geothermal cascade utilization has been implemented. The mining influence radius is generally less than 0.8 km, and the calculated boundary can be determined as the known head boundary, with the initial water level buried depth of 14.5 m. Additionally, hydrogeological parameters are important indexes to characterize the characteristics of aquifer, mainly including the permeability coefficient of water-bearing medium and the elastic water release coefficient of confined aquifer. Based on the pumping test data of the mining hole in the project, the permeability coefficient K = 0.09 m per day and the elastic water release coefficient μ^* = 0.0006 Lpm were determined.

Results and discussion

In the working process of GWHP system, the extraction of groundwater by the pumping well will cause the groundwater level in the aquifer to form an additional flow field, while the recharge well will recharge the aquifer and form a rising additional flow field. The influence of the GWHP system on the formation of underground-water flow system is actually the result of the superposition of the two additional flow fields. In this study, the two flow fields were simulated separately by numerical simulation under the condition of different recharge ratios, so as to quantitatively analyze and evaluate the influence of pumping and recharge on the regional groundwater system.

Change of water level of the observed well

The GWHP project of Fuyang People's Hospital is designed with four geothermal wells with an interval of 300 m between each adjacent well, which the 4 wells are numbered W1, W2, W3, and W4, respectively, are evenly arranged in the corner of the site. In order to understand the spatial variation of water level during the numerical simulation, three observation points, named obs. 1, obs. 2, and obs. 3, are set up in the project area. The plane lay-out is shown in fig. 1, obs. 1 is located outside the site and 100 m away from the nearest recharge well, obs. 2 is located in the center of the site, and obs. 3 is located outside the site and 100 m away from the nearest pumping well.

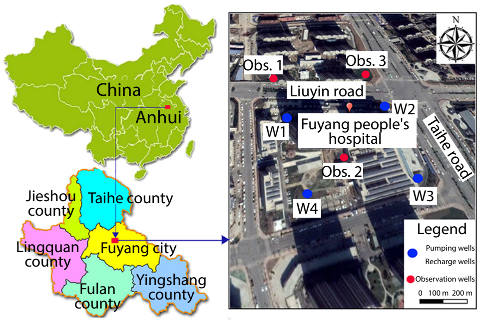

Figure 1. Study area and distribution of well group

In the simulation process, the initial water level of the model is 14.5 m, the water pumping capacity of a single well is 720 m^3 per day, so the total pumping capacity of two Wells is 1440 m^3 per day, which is then evenly distributed among two recharge wells. When the total volume of reinjection is 90% and 100% of the pumping volume, the groundwater level of obs. 1, obs. 2 and obs. 3 at three different calculation points near the well group changes dynamically, as shown in fig. 2.

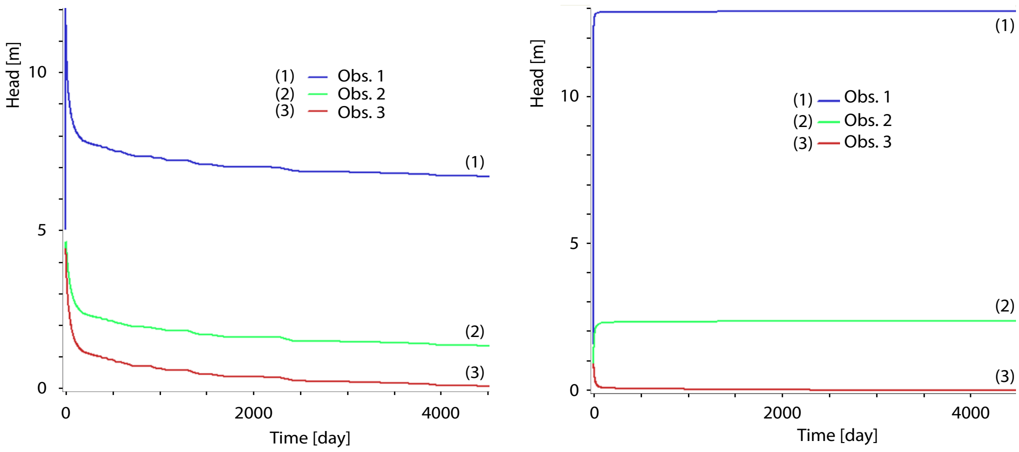

Figure 2. Dynamic curve of water level at observation point; (a) 90% recharge and (b) 100% recharge

Figure 2(a) shows that under the condition of 90% recharge, the water level the obs. 1 rose rapidly, with the maximum increase of 7.0 m. After that, it gradually stabilized at an increase of 2.2 m. At obs. 2, the water level gradually decreased and stabilized at a decrease of 3.3 m. obs. 3 gradually decreased and stabilized at 4.9 m. As shown in fig. 2(b), obs. 1 gradually stabilized after the water level rose rapidly to an increase of 11.0 m under 100% reinjection conditions. In the mean time, the water level of obs. 2 gradually rose and stabilized at an increase of 1.5 m. At obs. 3 site, which is characterized by a gradual decline in water level and a stabilization of 0.9 m.

Simulation analysis of different pumping and recharge modes

Under the condition of different recharge ratio, the water level of the observed well changes obviously. Therefore, the influence of pumping and recharge process on regional groundwater needs to be further studied. In the simulation, different recharge ratios and recharge modes are distinguished, and the influence of water level drawdown during continuous operation of GWHP and the water level recovery after stopping are analyzed.

Same direction recharge

Under the condition of W3 and W4 wells pumping water while W1 and W2 wells recharging water, the system has the greatest influence on the formation of groundwater flow field with the maximum production capacity of 1440 m^3 per day and the longest continuous operation period of 4 months. At the proportion of 90% and 100% same direction recharge, the groundwater flow field at the end of operation are as it is shown on fig. 3.

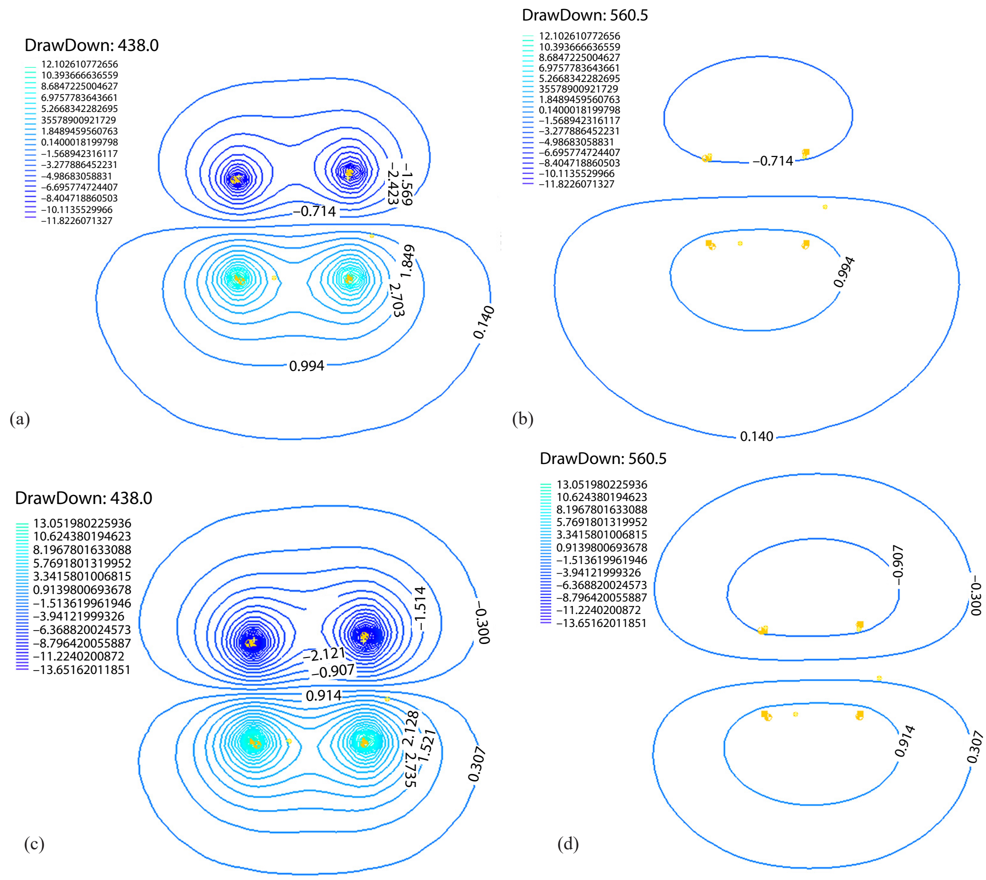

Figure 3. Drawdown distribution of groundwater flow field with same direction recharge; (a) four months operation with 90% recharge, (b) four months shutdown with 90% recharge, (c) four months operation with 100% recharge, and (d) four months shutdown with 100% recharge

As can be seen from fig. 3(a), a local groundwater cone of depression was formed near the group of pumping wells at the end of four months, the maximum influence range is about 0.40 km^2 (that is, the area of drawdown is greater than zero). The range of drawdown greater than 5 m, 3 m, and 1 m is about 0.02 km^2, 0.08 km^2, and 0.27 km^2, respectively, and the maximum drawdown is about 13.7 m near the center of pumping wells group. Correspondingly, a local water rise funnel zone is formed near the recharge wells, in which the range of drawdown greater than –5 m, –3 m, and –1 m is about 0.02 km^2, 0.06 km^2, and 0.17 km^2, respectively, and the maximum drawdown near the center of the recharge wells group is about –12.9 m. Figure 3(b) shows that the drawdown around the pumping well decreased by 0.99 m and the recharge wells group increased by 0.71 m when the system is stopped for four months, and the water level is basically restored to the pre-mining level after eight months.

It can be concluded from fig. 3(c) that the maximum influence which the range of drawdown greater than zero, is about 0.36 km^2. The range of drawdown greater than 5 m, 3 m, and 1 m is about 0.02 km^2, 0.07 km^2, and 0.25 km^2, respectively, and the maximum drawdown is about 13.4 m near the center of pumping wells. In the meantime, a rising funnel is formed near the recharge wells, where the area of drawdown greater than –5 m, –3 m, and –1 m is about 0.02 km^2, 0.08 km^2, and 0.28 km^2, respectively, and the maximum drawdown near the center of the recharge wells group is about –12.6 m. As show in fig. 3(d), after four months of the system shutdown, the drawdown around the pumping well decreased by 0.90 m and the recharge wells group increased by 0.91 m, and it was almost back to the pre-production level in eight months later.

Intersect recharge

Under the condition of W1 and W3 wells pumping water while W2 and W4 wells recharging water, the system has the greatest influence on the formation of groundwater flow field with the maximum production capacity of 1440 m^3 per day and the longest continuous operation period of four months. At the proportion of 90% and 100% Intersect direction recharge, the groundwater flow field at the end of operation are as it is shown in fig 4.

As can be seen from fig. 4(a), a partial drawdown funnel was formed near the group of pumping wells at the end of four months, the maximum influence range is about 0.30 km^2 (that is, the area of drawdown is greater than zero). The range of drawdown greater than 5 m, 3 m, and 1 m is about 0.03 km^2, 0.07 km^2, and 0.11 km^2, respectively, and the maximum drawdown is about 13.8 m near the center of pumping wells group. Correspondingly, a local water rise funnel zone is formed near the recharge wells, in which the range of drawdown greater than –5 m, –3 m, and –1 m is about 0.02 km^2, 0.05 km^2, and 0.09 km^2, respectively, and the maximum drawdown near the center of the recharge wells group is about –11.8 m. Figure 4(b) shows that the drawdown around the recharge wells group rose to 0.51 m when the system is stopped for four months, and the water level is basically restored to the pre-mining level after eight months.

From fig. 4(c), it can be concluded that the maximum influence which the range of drawdown greater than zero, is about 0.25 km^2. The range of drawdown greater than 5 m, 3 m, and 1 m is about 0.02 km^2, 0.06 km^2, and 0.10 km^2, respectively, and the maximum drawdown is about 13.7 m near the center of pumping wells. In the meantime, a rising funnel is formed near the recharge wells, where the area of drawdown greater than –5 m, –3 m, and –1 m is about 0.02 km^2, 0.07 km^2, and 0.11 km^2, respectively, and the maximum drawdown near the center of the recharge wells group is about –12.4 m. As show in fig. 4(d), after four months of the system shutdown, the drawdown around the recharge wells group rose to 0.45 m, and it was almost back to the pre-production level in eight months later.

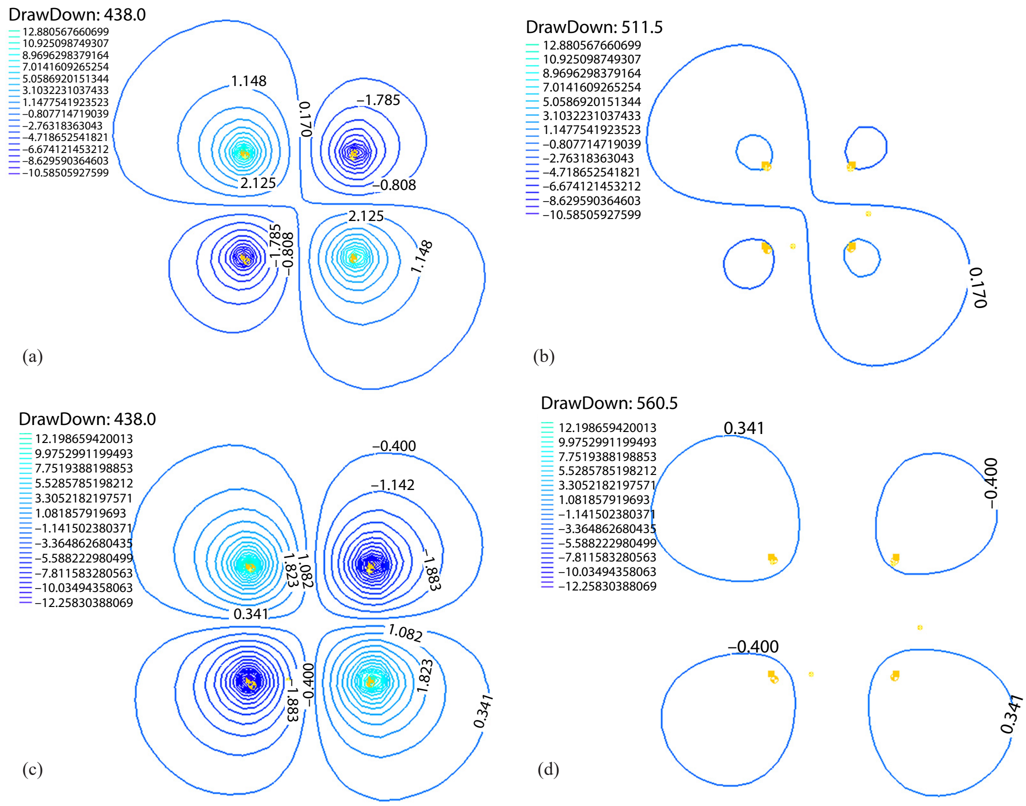

Figure 4. Drawdown distribution of groundwater flow field with intersect recharge; (a) four months operation with 90% recharge, (b) four months shutdown with 90% recharge, (c) four months operation with 100% recharge, and (d) four months shutdown with 100% recharge

Impact analysis of pumping and recharging

Based on the aforementioned two different pumping-recharge ratios and the lay-out of wells, the effect of GWHP project on regional groundwater during the maximum continuous operation period is shown in fig. 5. According to fig. 5, the area affected by different recharge patterns and recharge ratios decreases with the increase of the drawdown. For the pumping well, the funnel area under the 90% recharge is greater than that of 100%, when the draw-down drops to 1 m, the maximum funnel areas of 90% recharge are 0.27 km^2 and 0.11 km^2, respectively, which are greater than 0.25 km^2 and 0.10 km^2 under the 100% recharge. However, for recharge wells, the funnel area under 90% recharge is less than the area of 100% recharge, and when the drawdown drops to –1 m, the maximum funnel area of 90% recharge are 0.17

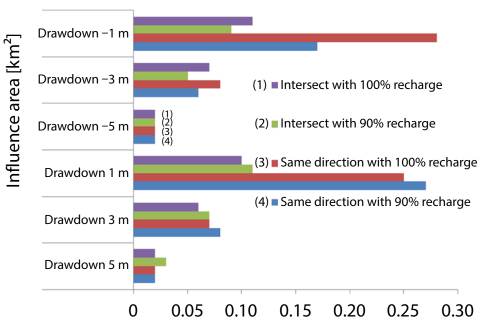

Figure 5. Comparison of funnel area of groundwater under different pumping and recharge modes

km^2 and 0.09 km^2, respectively, less than 0.28 km^2 and 0.11 km^2 under 100% recharge. The two kinds of influence changes are more obvious with the decrease of the depth, which is because with the increase of the water volume of the recharge well, the area affected by the rising water level is also increased. Furthermore, a part of groundwater in the recharge well flows back to the pumping well through the action of convection and dispersion [22, 23], which can supplement and balance the water of the pumping well and reduce the influence of the pumping well on the regional groundwater.

However, there are still some differences between different recharge patterns and recharge ratios: in pumping wells and recharge wells, the funnel area of 90% same direction recharge is larger than that of 90% intersect recharge, the funnel area of 100% same direction is larger than that of 100% intersect recharge, and with the decrease of the drawdown, the larger the difference in the range of effects.

Therefore, the intersect recharge model has less disturbance to regional groundwater, and is more suitable for well group lay-out in GWHP project. What is more, when the drawdown of pumping well is 1 m, the difference of funnel area between 90% same direction and intersect recharge is 0.16 km^2, and that of difference is 0.15 km^2 with 100% recharge. While the recharge well is reduced to –1 m, the difference of funnel area between 90% same direction and intersect recharge is 0.08 km^2, and the difference of 100% recharge is 0.17 km^2, so the regional influence range of the two models is smaller at the rate of 100% pumping recharge.

From the previous, considering the groundwater flow field, the intersect recharge mode with 100% recharge is preferred in the GWHP project. However, during the operation of the actual system, water leakage and natural loss of the unit still account for a certain proportion, the same direction and intersect recharge modes can be operated interchangeably after one cycle. Moreover, in order to minimize the influence of pumping and recharge systems on local groundwater, the pumping well and the recharge well are considered to be rotated year by year, which will also help to maintain the energy balance of the regional geothermal system.

Conclusions

- According to the dynamic change of water level of three observation points in the study area: under the condition of 90% and 100% recharge, the steady rise of water level of the observation points near the recharge well is 2.2 m and 11.0 m. While the observation point in the center of the site changes from 3.3 m to 1.5 m, and the observation point near the pumping well decreases steadily by 4.9 m and 0.9 m, respectively. Therefore, the response of groundwater level recovery to the recharge ratio of GWHP project is obvious.
- In the process of numerical simulation, when the GWHP operates at the maximum operating condition of 1440 m^3 per day and continuously for four months, a water-level drawdown funnel will be formed near the pumping well, while an inverted funnel of water-level rising will be formed near the recharge well, then, four months after the system shut down, the maximum water level of the pumping well decreased to 0.99 m, while the recharge well rose to 0.91 m, and the water level basically recovered after eight months. The characteristics of groundwater flow field in pumping well and recharge well indicate that the groundwater drawdown of GWHP project is in the state of dynamic equilibrium.
- Under different recharge modes and ratios, the area affected decreased with the increase of drawdown. However, the funnel area of the same direction recharge mode is larger than that of the intersect recharge in the same reinjection ratio in both pumping wells and recharge wells, and the difference of the funnel area is larger with the decrease of drawdown. In consequence, the intersect recharge mode is given priority in the well group lay-out of the

GWHP in order to reduce the disturbance to the regional groundwater. Moreover, with the increase of recharge amount, while the water level of recharge well rises, a part of groundwater flows back to the pumping well through convection and dispersion, so as to supplement and balance the water quantity of the pumping well.

Acknowledgment

This research work was supported by the key project of the Natural Science Foundation of Anhui (Grant No. KJ2017A409, 411), National Natural Science Foundation of China (Grant No. 51309071).

Nomenclature

C – average heat capacity of hot water, [$kJm^{-3}°C^{-1}$]
D – simulation area
H – groundwater level, [m]
H_0 – initial water level of groundwater, [m]
H_1 – groundwater level at the simulated boundary, [m]
K – aquifer hydraulic conductivity, [m per day]
M – thickness of confined aquifer, [m]
P – total heating load, [kW]
Q_d – water intake flow of hot well, [m^3 per day]
T_r – pumping temperature, [°C]
T_0 – recharge water temperature, [°C]
t – time, [day]
t_h – time, [h]
W – unit volume flow, [m^3]

Greek symbols

Γ_1 – the first class boundary of head loss
μ^* – elastic storage coefficient, [Lpm]
ρ – density of water, [1000 kgm^{-3}]

References

[1] Florides, G., *et al.*, Modelling and Assessment of the Efficiency of Horizontal and Vertical Ground Heat Exchangers, *Energy*, *58* (2013), Sept., pp. 655-663
[2] Wang, Z., *et al.*, Research of Heat and Moisture Transfer Influence on the Characteristics of the Ground Heat Pump Exchangers in Unsaturated Soil, *Energy Build*, *130* (2016), Oct., pp. 140-149
[3] Pulat, E., *et al.*, Experimental Study of Horizontal Ground Source Heat Pump Performance for Mild Climate in Turkey, *Energy*, *34* (2009), 9, pp. 1284-1295
[4] Ni, L., *et al.*, A review of Heat Pump Systems for Heating and Cooling of Buildings in China in the Last Decade, *Renew Energy*, *84* (2015), Dec., pp. 30-45
[5] Emmi, G., *et al.*, An Analysis of Solar Assisted Ground Source Heat Pumps in Cold Climates, *Energy Conversion and Management*, *106* (2015), Dec., pp. 660-675
[6] Ramos, E. P., *et al.*, Geothermal Heat Recovery from Abandoned Mines: A Systematic Review of Projects Implemented Worldwide and a Methodology for Screening New Projects, *Environmental Earth Sciences*, *73* (2015), Mar., pp. 6783-6795
[7] Huang, S., *et al.*, Strength and Failure Characteristics of Rock-Like Material Containing Single Crack under Freeze-Thaw and Uniaxial Compression, *Cold Regions Science and Technology*, *162* (2019), June, pp. 1-10
[8] Li, C., *et al.*, Numerical Simulation of Horizontal Spiral-Coil Ground Source Heat Pump System: Sensitivity Analysis and Operation Characteristics, *Applied Thermal Engineering*, *110* (2016), Jan., pp. 424-435
[9] Ferguson, G., Characterizing Uncertainty in Groundwater-Source Heating and Cooling Projects in Manitoba, *Canada, Energy*, *37* (2012), 1, pp. 201-206
[10] Liang, J., *et al.*, Modelling and Performance Evaluation of Shallow Ground-Water Heat Pumps in Beijing plain, China, *Energy Build*, *43* (2011), 11, pp. 3131-3138
[11] Shen, S. L., *et al.*, Calculation of Head Difference at Two Sides of a Cut-off Barrier during Excavation Dewatering, *Computers and Geotechnics*, *91* (2017), Nov., pp. 192-202
[12] Noorollahi, Y., *et al.*, The Effects of Ground Heat Exchanger Parameters Changes on Geothermal Heat Pump Performance – A Review, *Applied Thermal Engineering*, *129* (2017), Jan., pp. 1645-1658
[13] Sarbu, I., Sebarchievici, C., General Review of Ground-Source Heat Pump Systems for Heating and Cooling of Buildings, *Energy Build*, *70* (2014), Feb., pp. 441-454
[14] Ikeda, S., *et al.*, Optimization Method for Multiple Heat Source Operation Including Ground Source Heat Pump Considering Dynamic Variation in Ground Temperature, *Applied Energy*, *193* (2017), May, pp. 466-478

[15] Huchtemann, K., Muller, D., Combined Simulation of a Deep Ground Source Heat Exchanger and an Office Building, *Energy Build*, *73* (2014), Mar., pp. 97-105
[16] Noorollahi, Y., *et al*., Numerical Simulation of Power Production from Abandoned oil Wells in Ahwaz Oil Field in Southern Iran, *Geothermics*, *55* (2015), May, pp. 16-23
[17] Zhang, L., *et al*., A Transient Quasi-3-D Entire Time Scale Line Source Model for the Fluid and Ground Temperature Prediction of Vertical Ground Heat Exchangers (GHE), *Applied Energy*, *170* (2016), C, pp. 65-75
[18] Zarrella, A., *et al*., Analysis of Operating Modes of a Ground Source Heat Pump with Short Helical Heat Exchangers, *Energy Conversion and Management*, *97* (2015), June, pp. 351-361
[19] Bidarmaghz, A., *et al*., The Importance of Surface Air Temperature Fluctuations on Long-Term Performance of Vertical Ground Heat Ex-Changers, *Geomechanics for Energy and the Environment*, *6* (2016), June, pp. 35-44
[20] Wang, Z. H., *et al*., Field Test and Numerical Investigation on the Heat Transfer Characteristics and Optimal Design of the Heat Exchangers of a Deep Borehole Ground Source Heat Pump System, *Energy Conversion and Management*, *153* (2017), Dec., pp. 603-615
[21] Li, C. F., *et al*., Numerical Simulation of Ground Source Heat Pump Systems Considering Unsaturated Soil Properties and Groundwater Flow, *Applied Thermal Engineering*, *139* (2018), July, pp. 307-316
[22] Wang, Y., *et al*., Investigation of the Influence of Groundwater Seepage on the Heat Transfer Characteristics of a Ground Source Heat Pump System with a 9-Well Group, *Building Simulation*, *12* (2019), Apr., pp. 857-868
[23] Zhou, X. Z., Gao, Q., Experiment on the Relevance of Thermal Breakthrough between Pumping and Injecting Well Groups with Aquifer Advection, *Building Science*, *28* (2012), 5, pp. 189-194

Paper submitted: June 14, 2020
Paper revised: August 23, 2020
Paper accepted: September 17, 2020